# Supporting Information

## Donor-Acceptor Based Two- Dimensional Polymer as Supercapacitor Electrode with Long Cycling Stability

Bhagyasree T. M.,[a] Priyanka Pandinhare Puthiyaveetil,[b,c] Viksit Kumar,[a,b] Kiran Asokan,[a,b] K. Sreekumar,[b,c] Sukumaran Santhosh Babu*[a,b]

[a] Organic Chemistry Division, National Chemical Laboratory (CSIR-NCL), Dr. Homi Bhabha Road, Pune-411 008, India.
[b] Academy of Scientific and Innovative Research (AcSIR), Ghaziabad-201 002, India.
[c] Physical and Materials Chemistry Division, National Chemical Laboratory (CSIR-NCL), Dr. Homi Bhabha Road, Pune-411 008, India.

# General Information

Chemicals, 4,4',4"-nitrilotribenzaldehyde (**NTB**) having 95% purity commercially purchased from BLD Pharmatech Ltd., and [1,1'-Biphenyl]-4,4'-diamine purchased from Chempure and used as received. Oleum (30%), 1-butanol and 1,2-Dichlorobenzene (Spectrochem) were used as received.

# Experimental

The $^{1}H$, $^{13}C$ NMR spectra were recorded on a Bruker400 and 500 MHz NMR spectrometer. The chemical shift values for $^{1}H$ (TMS as internal standard) and $^{13}C$ NMR are recorded in DMSO-$d_6$. The value of the coupling constant (*J*) is stated in Hertz (Hz). All spectra were obtained at room temperature unless otherwise specified. The splitting of peaks is described as *s* (singlet), *d* (doublet), *dd* (doublet of doublets). The solid-state $^{13}C$ NMR spectrum was recorded on a Bruker-300 MHz NMR spectrometer instrument. FT-IR spectra were obtained on Perkin Elmer Spectrum Two spectrophotometer in 4000-400 $cm^{-1}$ range with a resolution of 4 $cm^{-1}$. The scanning electron microscope images were obtained using FEI, QUANTA 200 3D SEM instrument operating at 10, 15, and 20 kV, using tungsten filament as electron source, and before imaging, the samples were sputtered with gold by using SCD 040 Balzers Union sputtered. High-resolution images are captured by a high-resolution transmitted electron microscope (JEOL JEM 2200FES). X-ray photoelectron spectroscopy (XPS) analyses were performed on a Thermo Fisher Scientific Instruments UK, Sr.No.-KAS2020 with a Aluminium Kα+.The wide-angle X-ray diffraction (WAXD) analysis was recorded on a Rigaku, MicroMax-007HF equipped with a high-intensity Micro focus rotating anode X-ray generator. The data was collected with the help of Control Win software. A Rigaku, R-axis IV++ detector was used for the wide-angle experiments using Cu Kalpha (1.54 Å) radiation outfitted with a Ni filter, and an Aluminum holder was used as a sample holder. BET adsorption experiment (up to 1 bar) was performed on a Quantachrome Quadrasorb automatic volumetric instrument. The pore diameter was calculated by nonlocal density functional theory (NLDFT). Powder X-ray diffraction (PXRD) patterns were recorded on Phillips PANalytical diffractometer for Cu Kα radiation ($\alpha$ = 1.5406 Å), with a scan speed of 1° $min^{-1}$ and a step size of 0.02° in 2$\theta$. The electrochemical experiments were carried out using Biologic (VMP 300) potentiostat.

**Electrode fabrication.**

The working electrode of the study was prepared by varying different weight percentages of YP-50F Carbon as the conducting addictive's (15wt%, 25wt%, 50wt %). So the composition of the electrode, where 15 wt% YP-50F is added, is 80wt% active material: 15wt% YP-50F: 5wt% Polyvinylidene fluoride (PVDF). The other two electrode composition for the study was taken as 70wt%:25wt%:5wt% and 45wt%:50wt%:5wt%, which is dispersed in N-methyl pyrrolidone (NMP) solvent. The viscous slurry obtained after 3h sonication drop-casted over GRAFOIL current collector. The electrodes were dried in an oven at 60 $^{o}$C overnight. The total mass loading over the electrode was 1 mg/cm$^2$.

**Electrochemical measurements.**

The **NTB-DBT** electrode is employed as a working electrode. Pt mesh and $Hg/Hg_2SO_4$ served as counter and reference electrodes, respectively, and 1M $H_2SO_4$ was the electrolyte. The electrochemical performance of the material is evaluated through cyclic voltammetry (CV) and galvanostatic charge-discharge (GCD) measurements. The potential window was fixed between -0.7 to 0.23 V vs. $Hg/Hg_2SO_4$.

**Equations and calculations used for electrochemical performance evaluation.**

(A) Calculation of specific capacitance (Csp) from chrono charge-discharge method is given in equation 1.

$$C_{sp} = \frac{(I*\Delta t)}{(Z*\Delta V)} \qquad \ldots\ldots \quad (1)$$

*C*sp is the specific capacitance (F g$^{-1}$)

I is the current used for charging and discharging

Z is the total mass loading

$\Delta$V is the potential window

$\Delta$t is the discharge time (sec)

For the calculation of specific capacitance of the device, equation 1 is used, where Z is taken as the total mass loading in both electrodes.

To find the single electrode capacitance, the above equation should be multiplied by 4.

The energy density and power density of the materials were calculated by the following equations:

$$E = C\text{sp} * \frac{\Delta V^2}{7.2} \quad \text{.....(2)}$$

$$P = E * \frac{3600}{\Delta t} \quad \text{.....(3)}$$

*E* is the energy density (in Wh $kg^{-1}$)

P is the power density (in W $kg^{-1}$)

$\Delta t$ is the total discharge time (in sec)

# Synthesis and Characterization

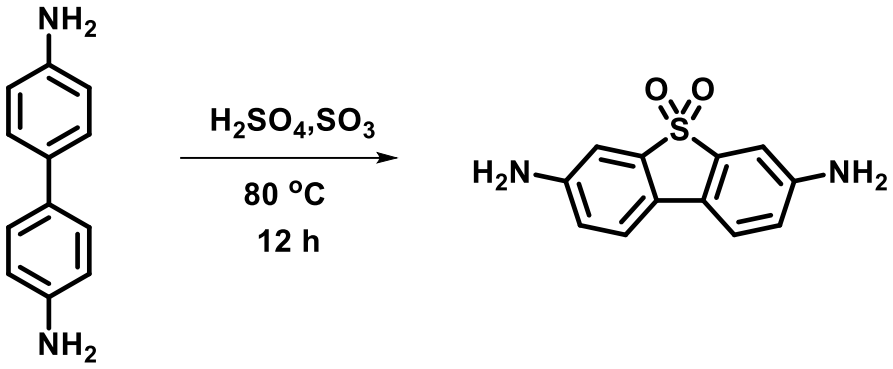


**Scheme S1**: Synthesis of 3,7-diaminodibenzo[*b*,*d*]thiophene sulfone (**DBT**).[S1]

**3,7-Diaminodibenzo[*b*,*d*]thiophene sulfone:** [1,1'-Biphenyl]-4,4'-diamine (2.46 g, 10 mmol) was taken up in sulfuric acid (5 mL, 30% free $SO_3$) and formed brown solution was heated to 80 °C overnight. After cooling to room temperature, the black mixture was poured into ice water and neutralized with saturated sodium bicarbonate solution. After drying at 80 °C, the product was obtained as a green powder (1.2 g, 48%).

$^1$H NMR (400 MHz, DMSO-$d_6$) $\delta$ [ppm]: 7.51 (d, $J$ = 8.38 Hz, 2H), 6.88 (d, $J$ = 2.13 Hz, 2H), 6.80 – 6.78(dd, $J$ = 8.26 Hz, $J$ = 2.13 Hz 2H) 5.73 (s, 4 H).

$^{13}$C NMR (100 MHz, DMSO-$d_6$) $\delta$ [ppm]: 149.8, 137.9, 121.9, 119.9, 118.9, 105.8. $^{135}$DEPT NMR (100 MHz, DMSO-$d_6$) $\delta$ [ppm]: 121.9, 118.9, 105.8.

**Synthetic scheme for the preparation of NTB-DBT**

4,4',4"-nitrilotribenzaldehyde **NTB** (22.07 mg, 0.66 eq), 3,7-Diaminodibenzo[b,d]thiophene sulfone **DBT** (25 mg, 1 eq), glacial acetic acid (6M, 0.6 eq), *n*-BuOH:*o*-DCB mixture (3 mL, 3:7) were taken in a pyrex tube and degassed. Followed by three freeze-pump-thaw cycles, the tube was vacuum-sealed off. The reaction mixture was heated at 120 °C for 3 days. 2D sheets were precipitated and collected by centrifugation. Polymer washed with distilled methanol and soxhlet extraction with acetone, $CH_2Cl_2$, and THF, respectively. The obtained dark purple fluffy material dried at 110 °C under vacuum for 12 h.[S1,S2]

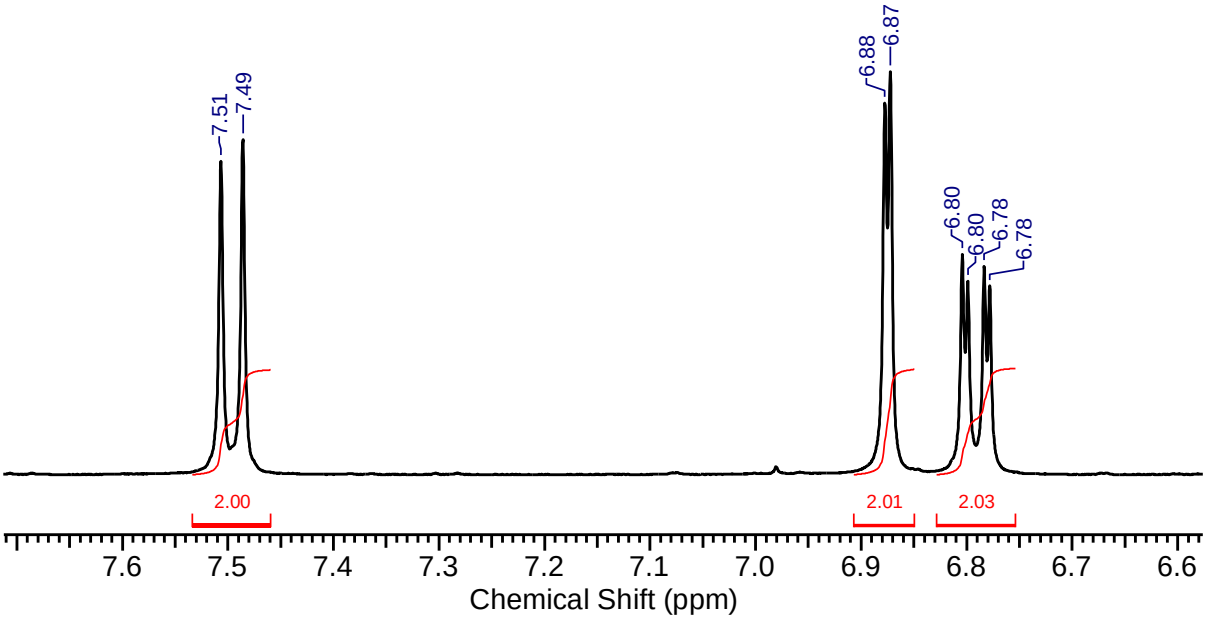


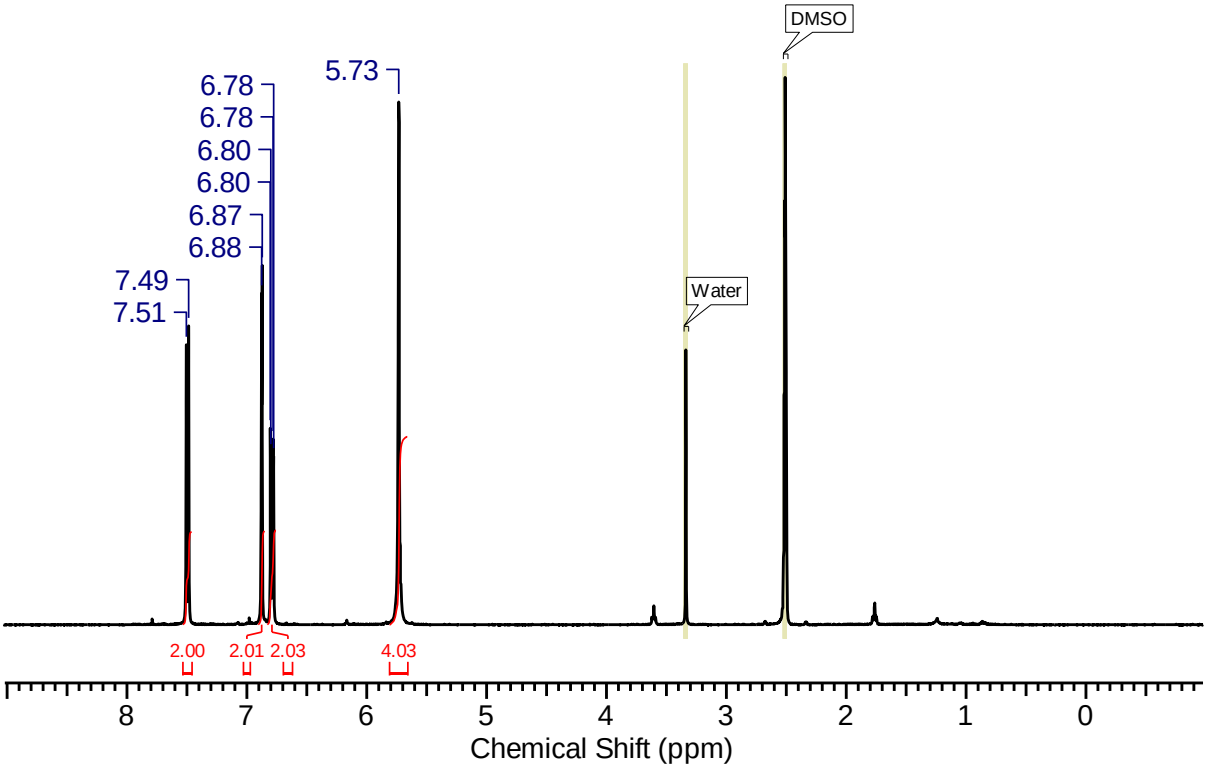


$^{1}$H NMR spectrum of **DBT**.

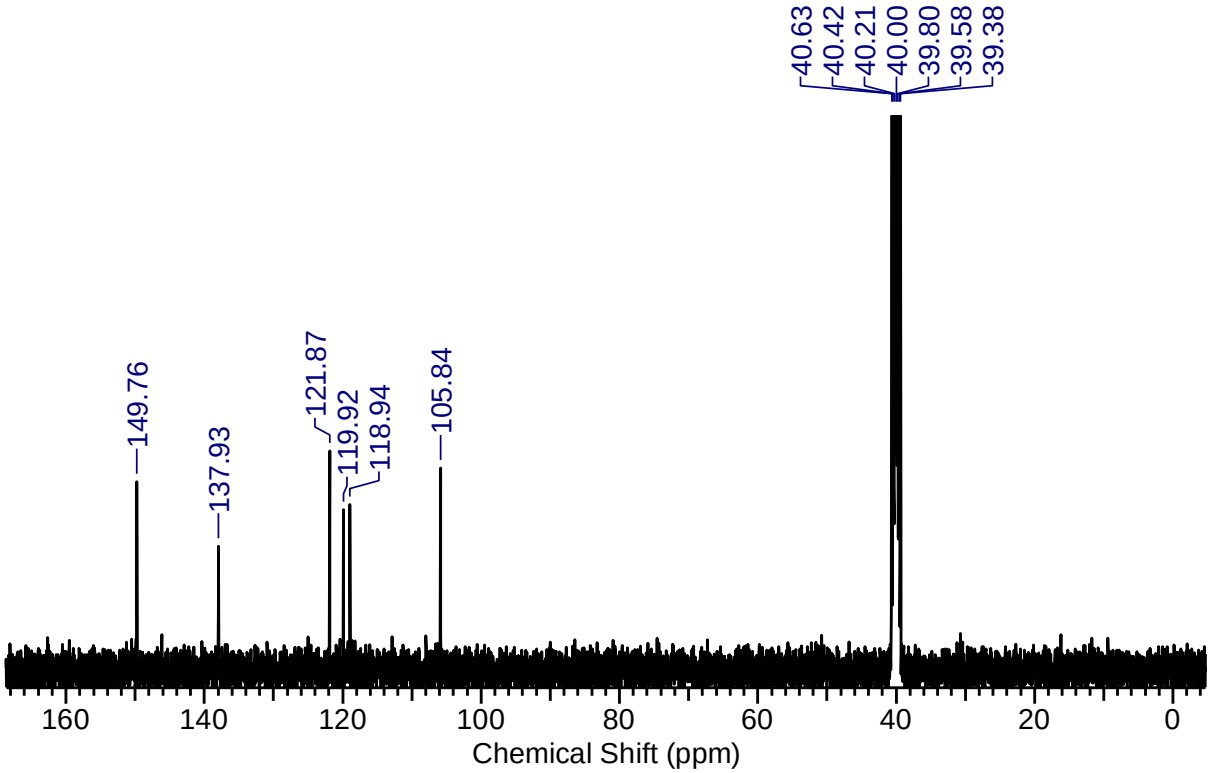


$^{13}$C (100 MHz) NMR spectrum of **DBT** in DMSO-$d_6$ at 298 K.

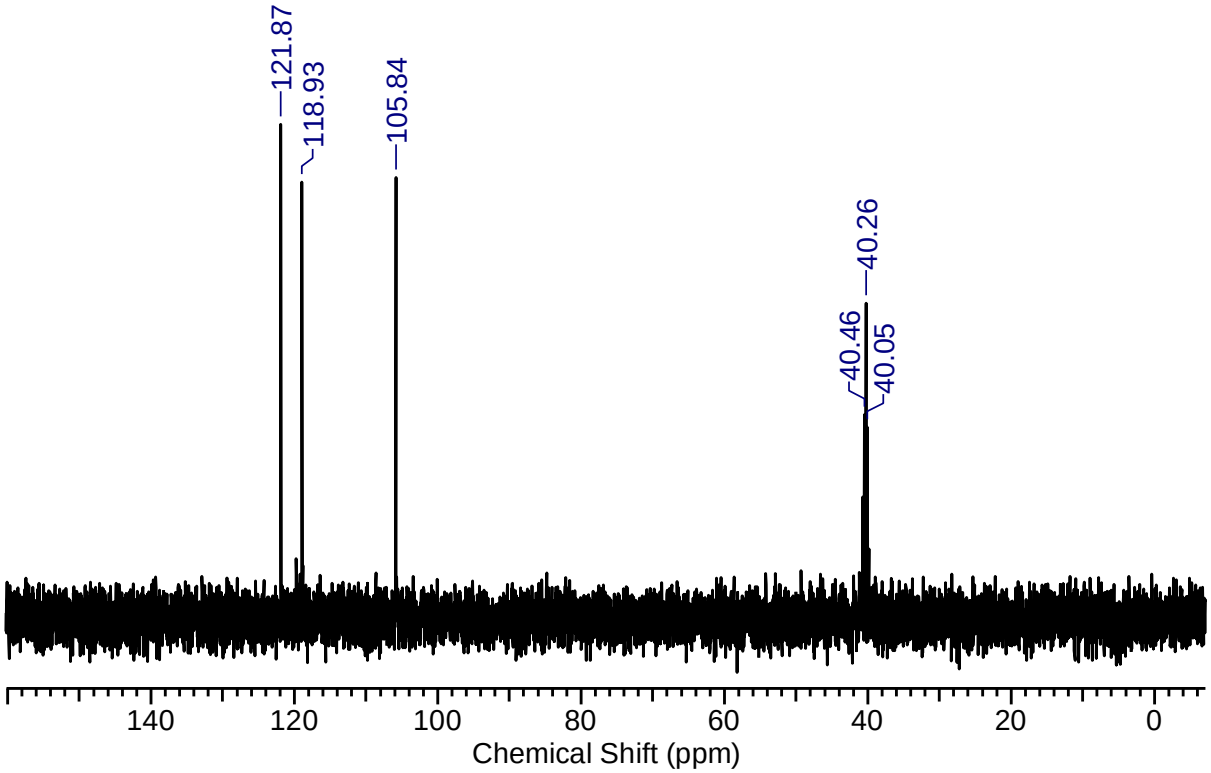


DEPT-135 (100 MHz) NMR spectrum of **DBT** in DMSO-$d_6$ at 298 K.

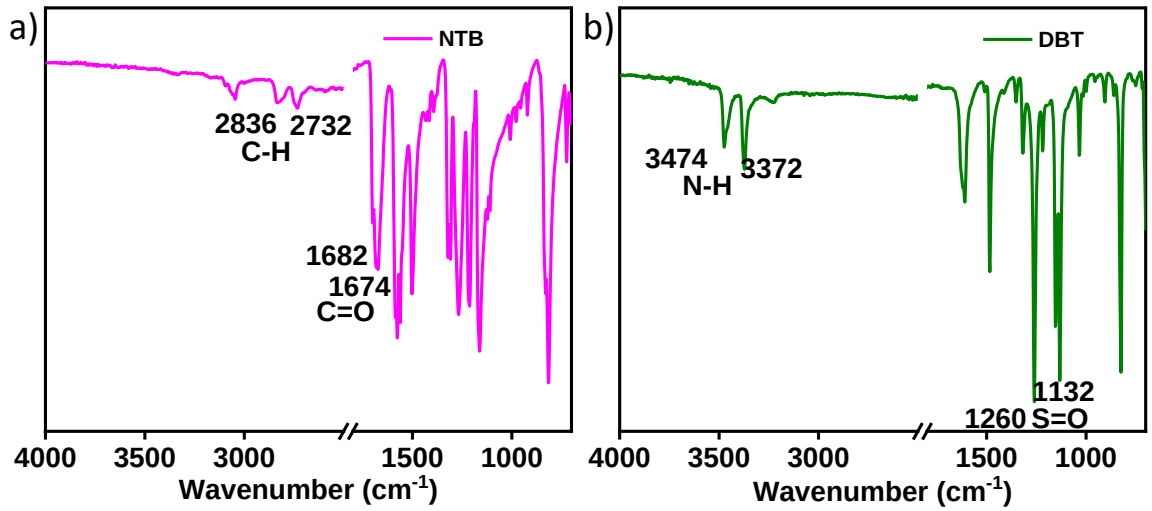


**Figure S1:** FT-IR spectra of a) **NTB** and b) **DBT**.

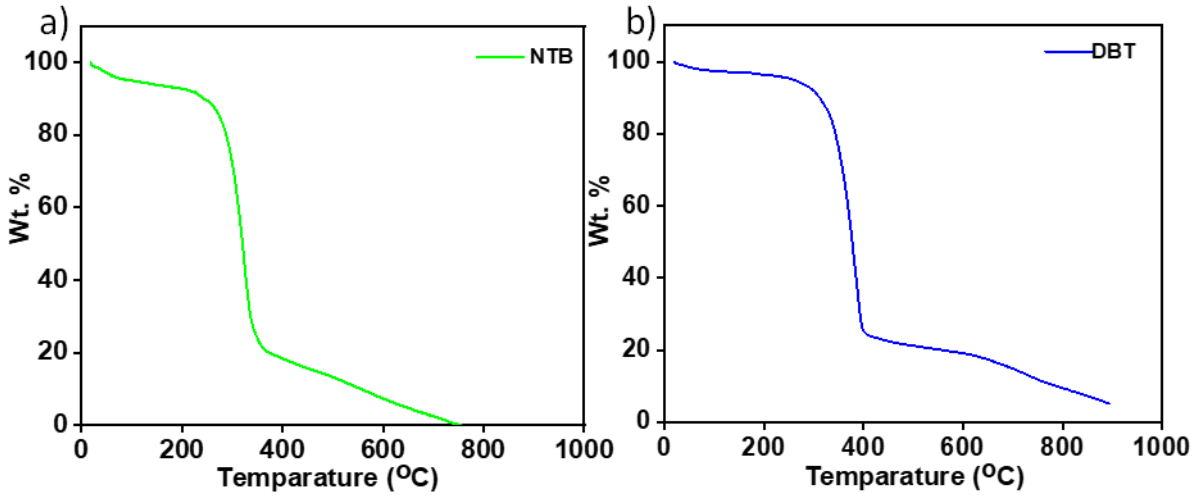


**Figure S2:** TGA spectra of a) **NTB** and b) **DBT**.

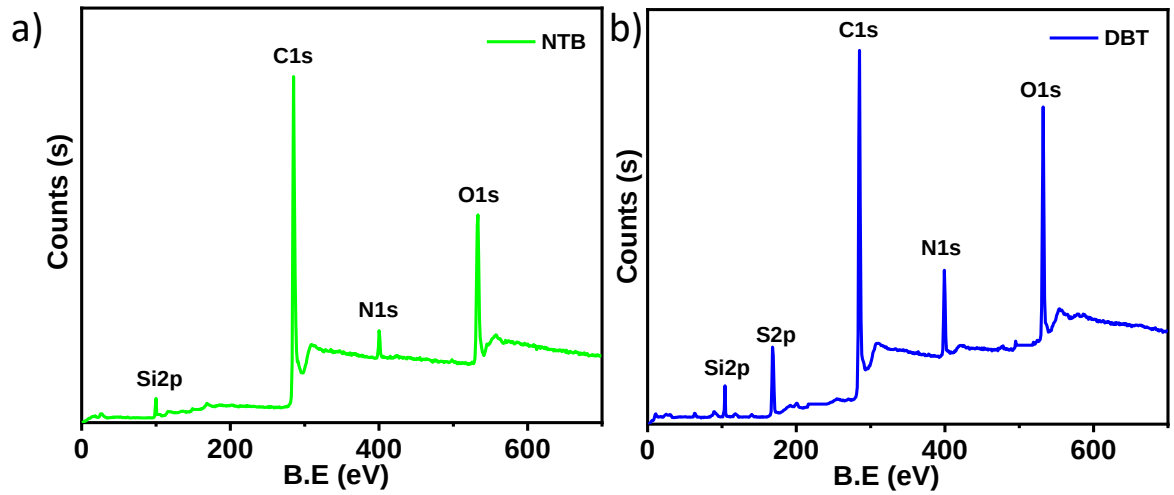


**Figure S3:** XPS spectra of a) **NTB** and b) **DBT**.

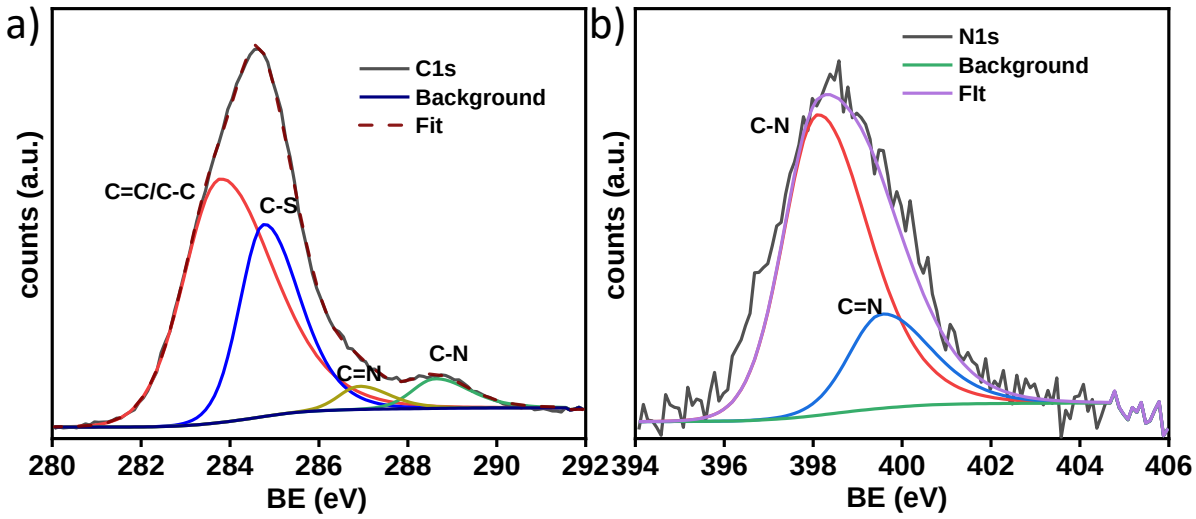


**Figure S4:** XPS of **NTB-DBT** a) C1s and b) N1s.[S3-5]

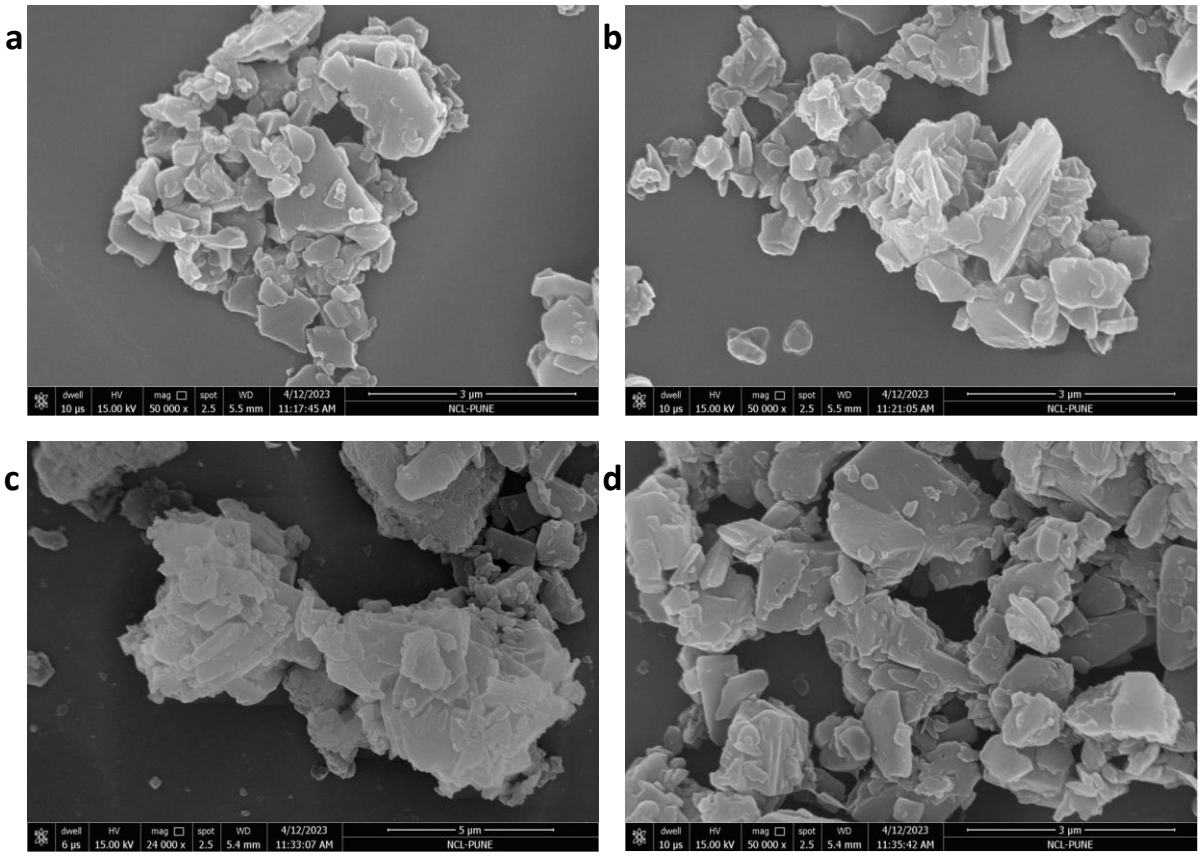


**Figure S5:** FE-SEM images of **NTB-DBT**.

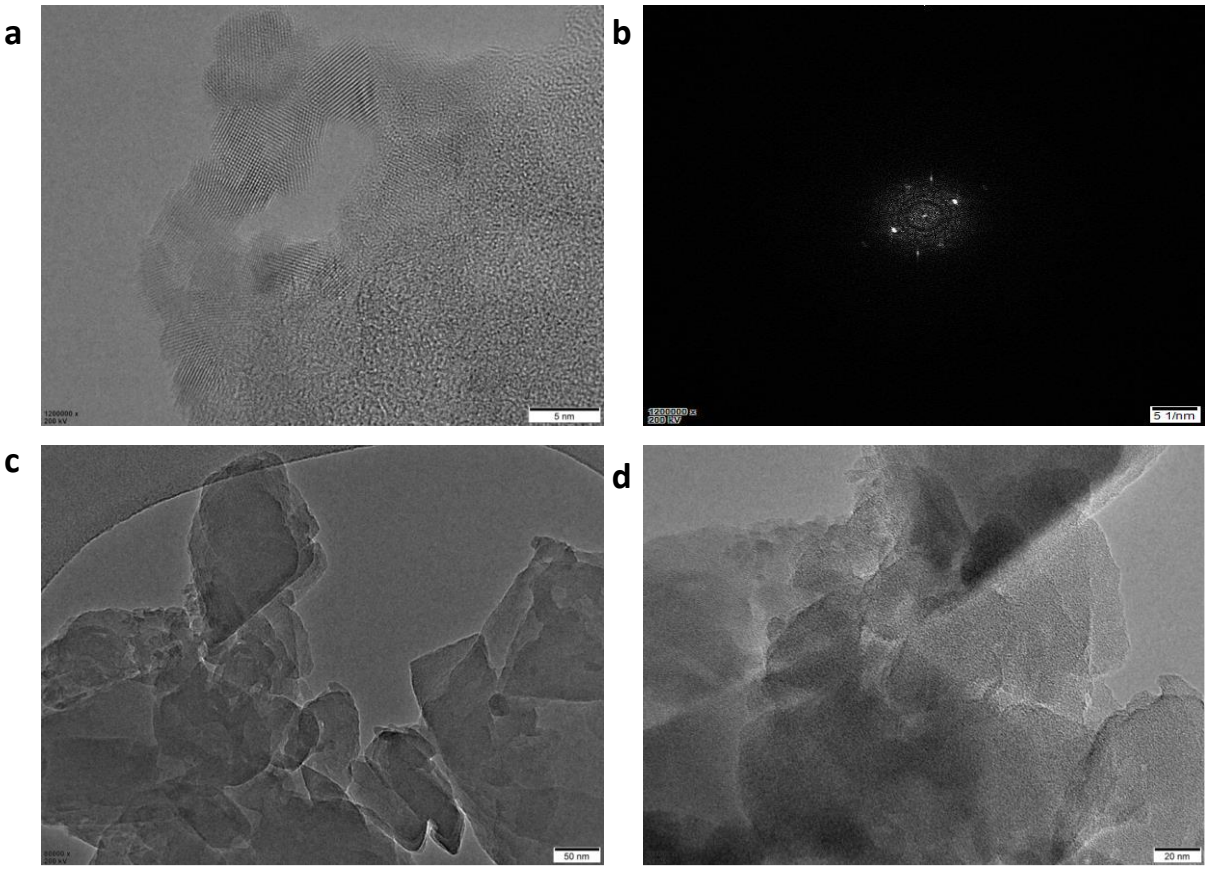


**Figure S6:** HR-TEM images of **NTB-DBT**.

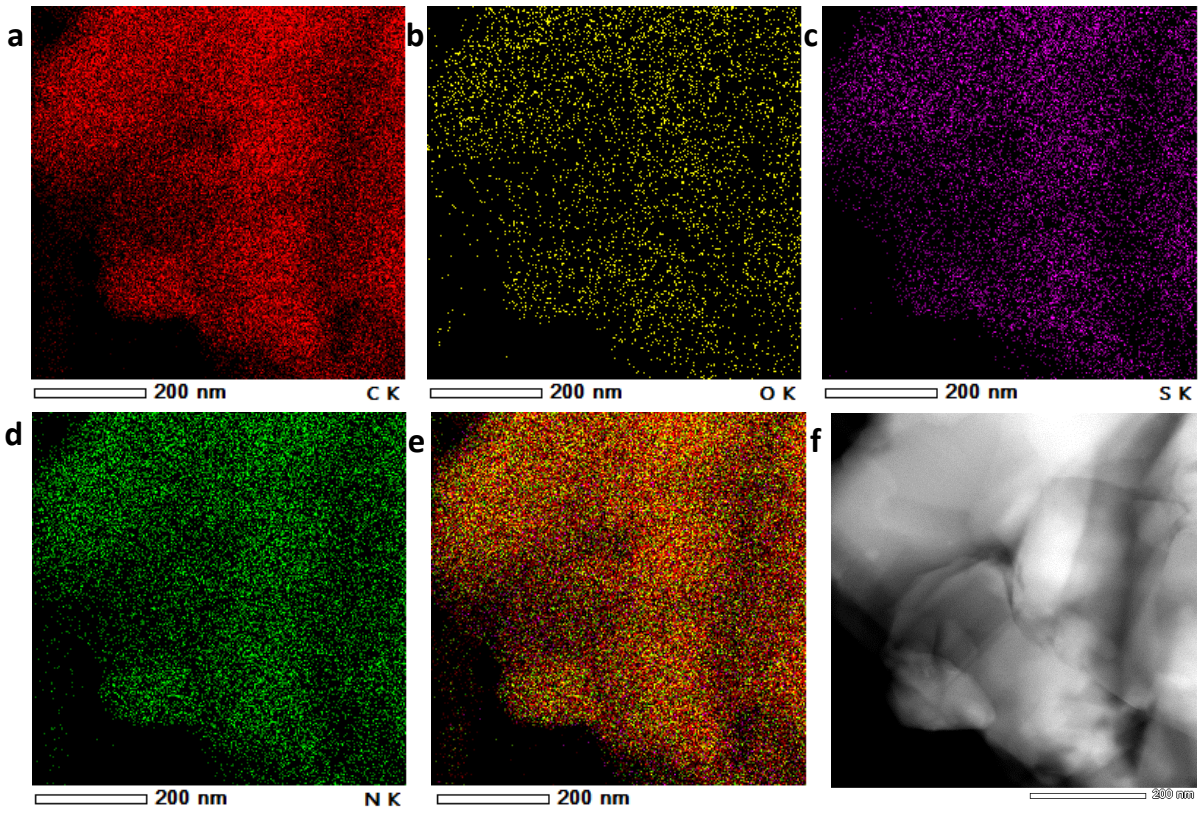


**Figure S7:** Elemental mapping of **NTB-DBT**.

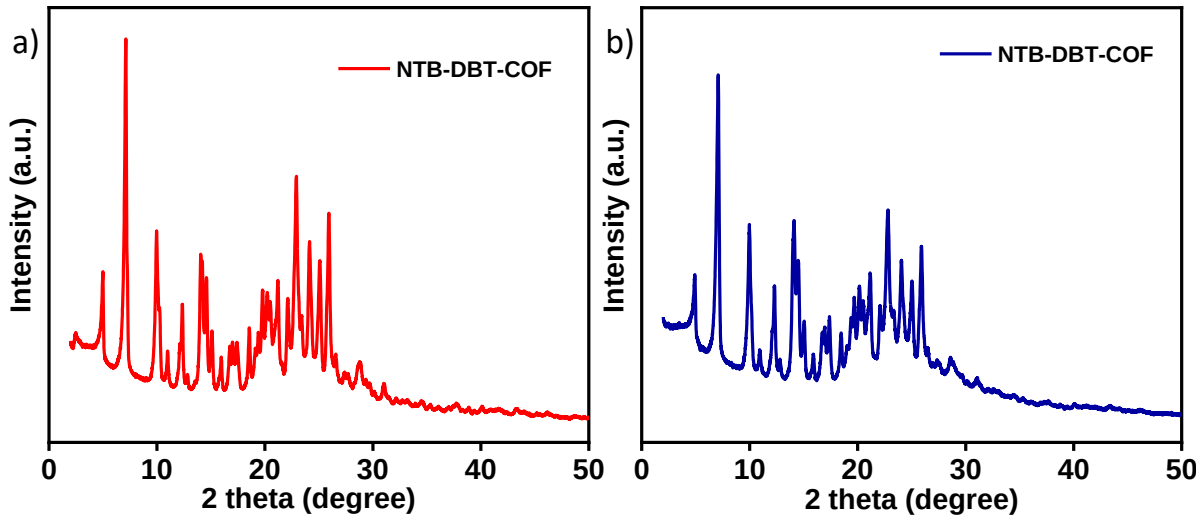


**Figure S8:** PXRD pattern of **NTB-DBT** in different solvents a) *o*-DCB/*n*-BuOH (7:3) and b) mesitylene/1,4-dioxane (1:1).

## Electrochemical Measurements

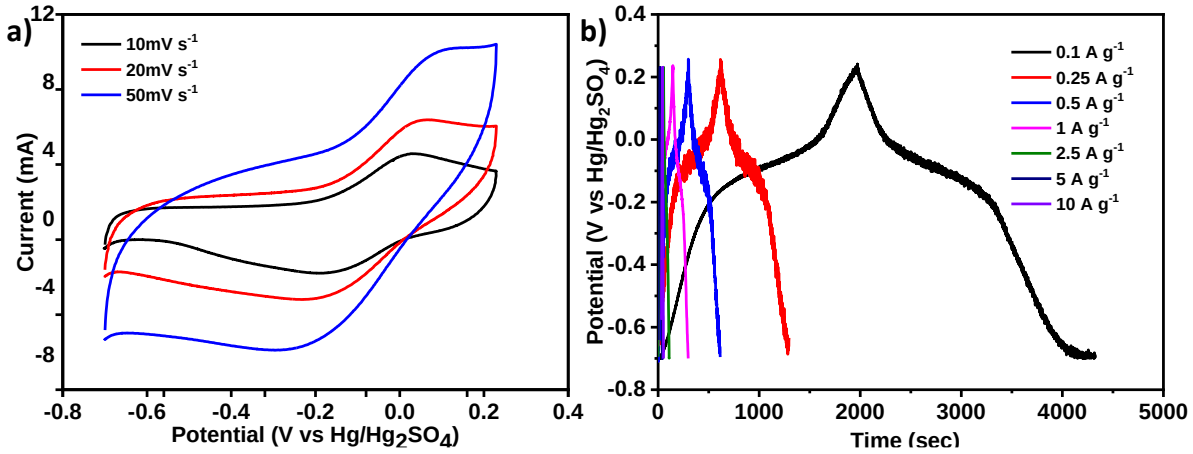


**Figure S9**. Electrochemical performance of the **NTB-DBT-70** in 1.0 M $H_2SO_4$ solution a) CV plot of the **NTB-DBT-70** at a scan rate of 10, 20, 50 mV $s^{-1}$ and b) GCD plot of the **NTB-DBT-70** at 0.1, 0.25, 0.5, 1, 2.5, 5, 10 A $g^{-1}$.

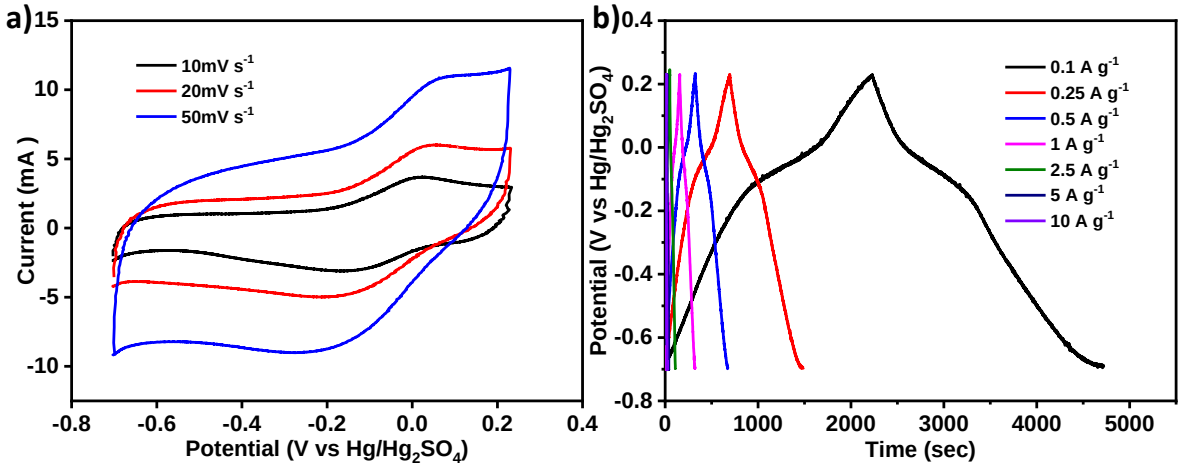


**Figure S10**. Electrochemical performance of the **NTB-DBT-45** in 1.0 M $H_2SO_4$ solution a) CV plot of the **NTB-DBT-45** at a scan rate of 10, 20, 50 mV $s^{-1}$ and b) GCD plot of the **NTB-DBT-45** at 0.1, 0.25, 0.5, 1, 2.5, 5, 10 A $g^{-1}$.

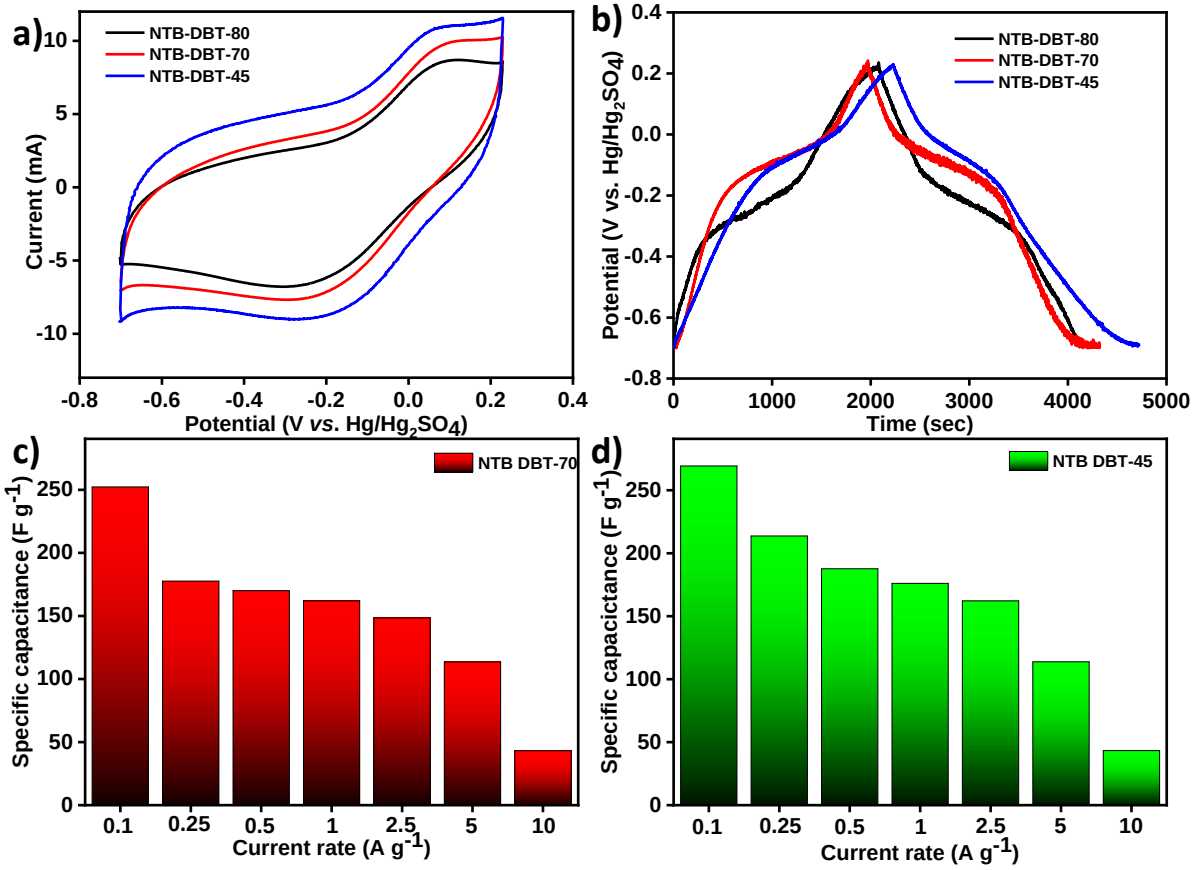


**Figure S11**. Electrochemical performance of the **NTB-DBT** in 1.0 M $H_2SO_4$ solution a) CV comparison plot of the **NTB-DBT-80**, **NTB-DBT-70**, and **NTB-DBT-45** at a scan rate of 50 mV $s^{-1}$, b) GCD comparison plot of the **NTB-DBT-80**, **NTB-DBT-70**, and **NTB-DBT-45** at the current rate of 0.1 A $g^{-1}$, c) specific capacitance of the **NTB-DBT-70** at 0.1, 0.25, 0.5, 1, 2.5, 5, 10 A $g^{-1}$, d) specific capacitance of the **NTB-DBT-45** at 0.1, 0.25, 0.5, 1, 2.5, 5, 10 A $g^{-1}$.

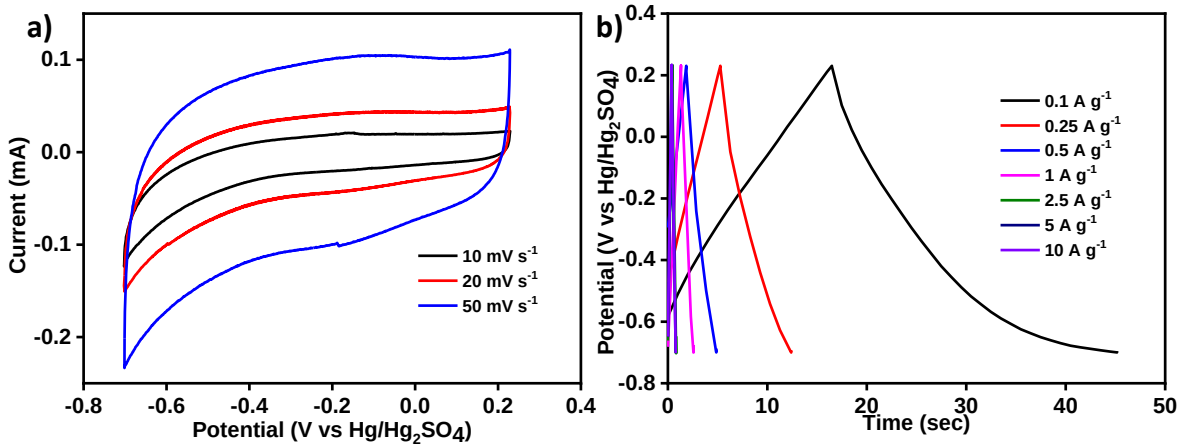


**Figure S12**. Electrochemical performance of the **YP-50F** in 1.0 M $H_2SO_4$ solution a) CV plot at a scan rate of 10, 20, 50 mV $s^{-1}$ and b) GCD plot at 0.1, 0.25, 0.5, 1, 2.5, 5, 10 A $g^{-1}$.

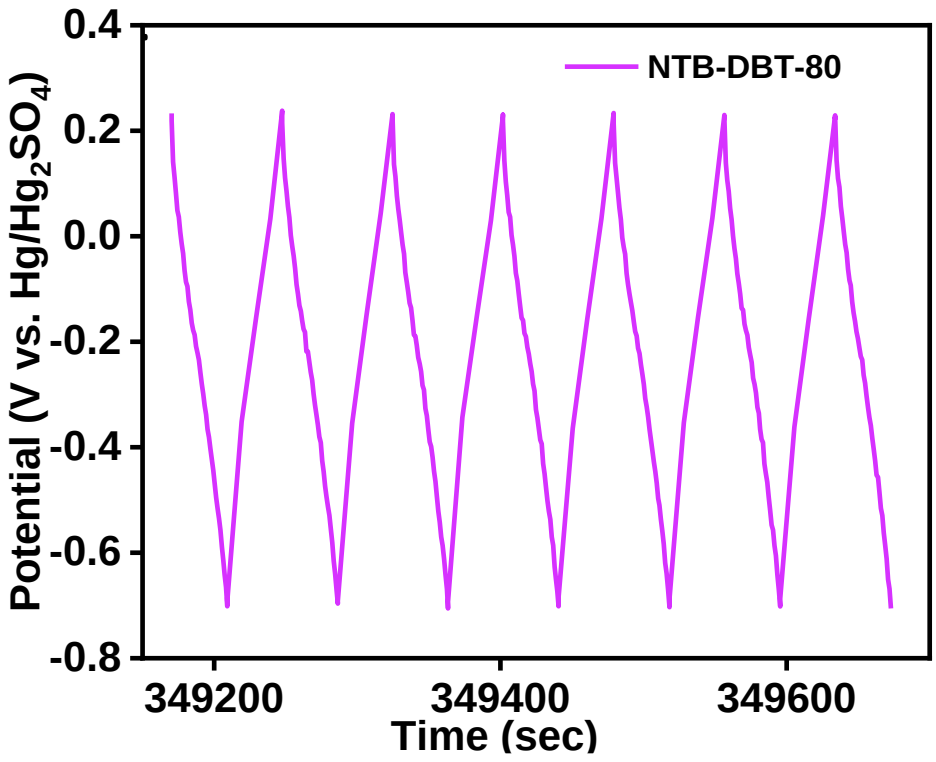


**Figure S13.** Potential vs. time plot of **NTB-DBT-80** in 1.0 M $H_2SO_4$ solution.

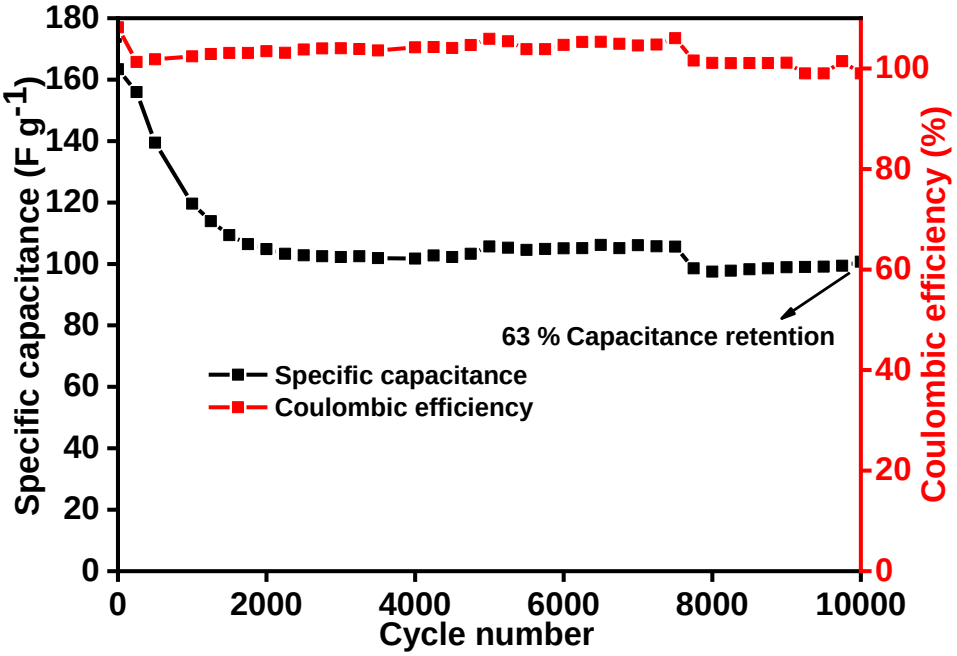


**Figure S14**. Cycling stability plot of the **NTB-DBT-70** at the current rate of 2.5 $Ag^{-1}$ in 1.0 M $H_2SO_4$ solution.

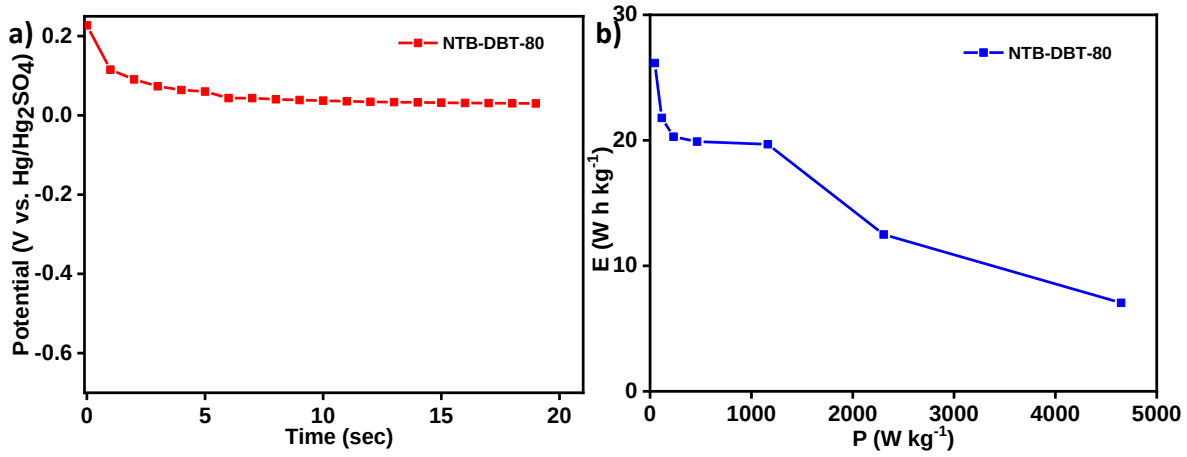


**Figure S15.** a) Self-discharge plot and b) Ragone plot of **NTB-DBT-80** in 1.0 M $H_2SO_4$ solution.

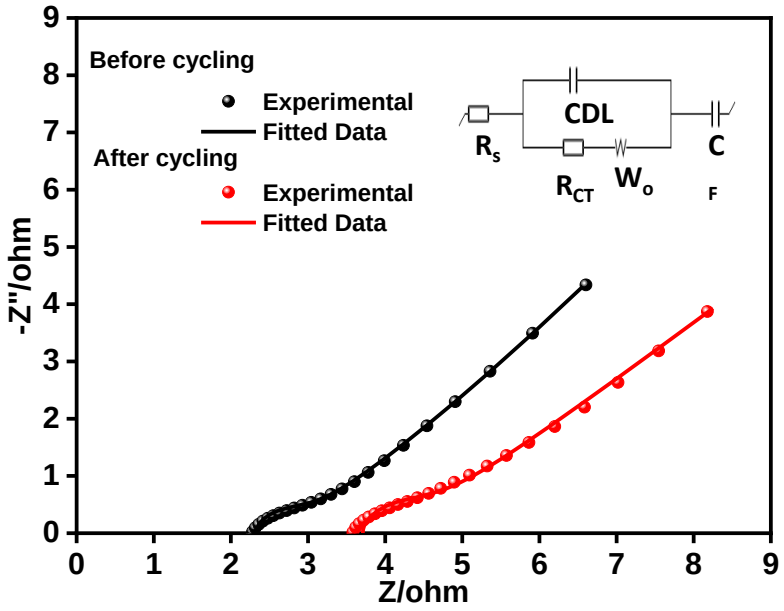


**Figure S16.** Nyquist plot of **NTB-DBT-80**-based symmetric supercapacitor.

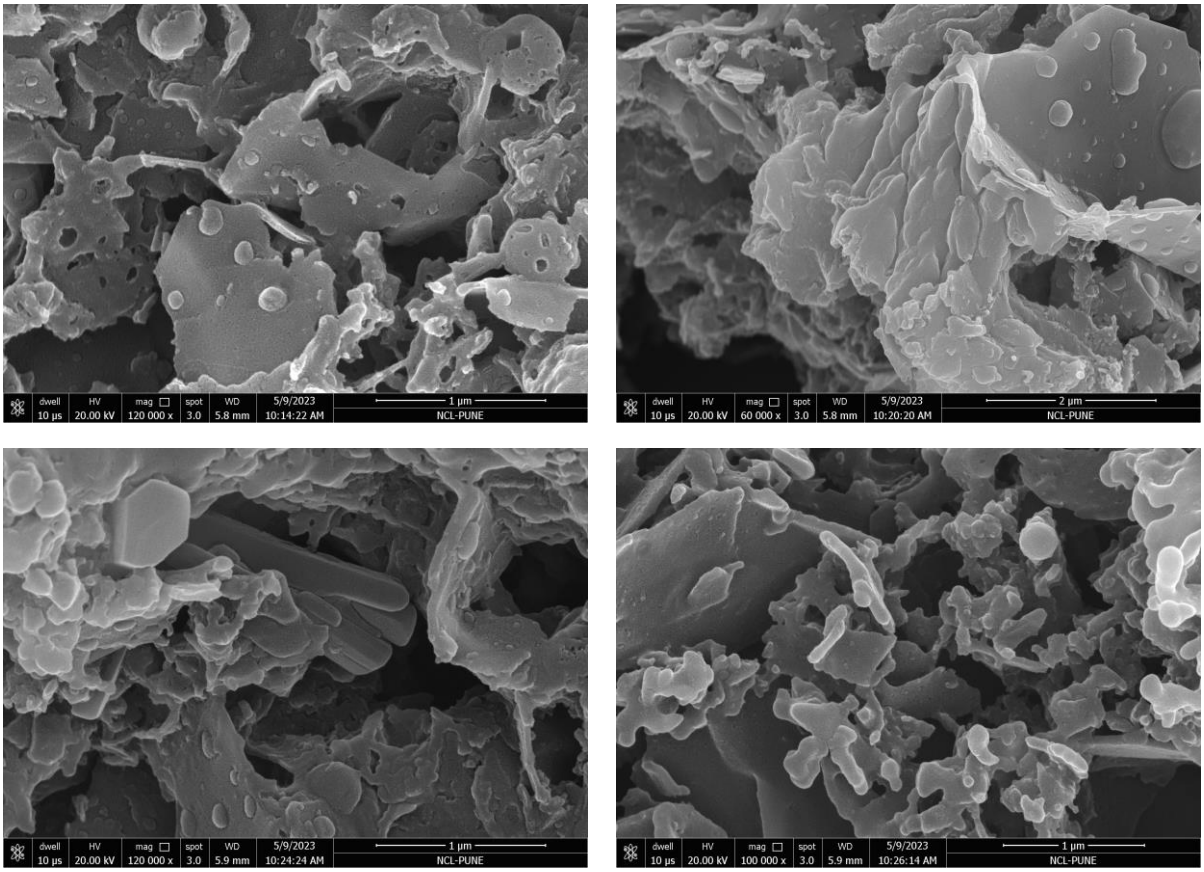


**Figure S17.** FE-SEM images of **NTB-DBT-80** after electrochemical studies.

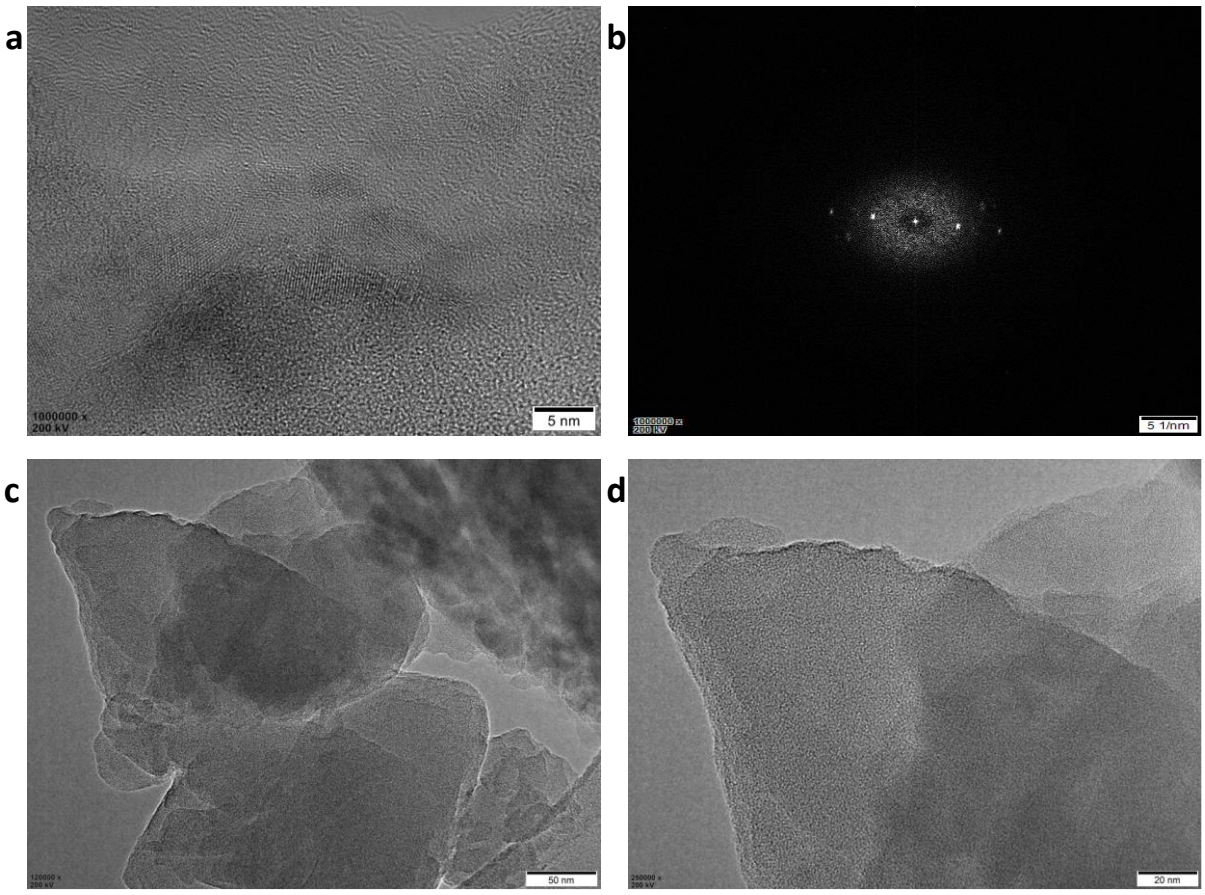


**Figure S18:** HR-TEM images of **NTB-DBT-80** after electrochemical studies.

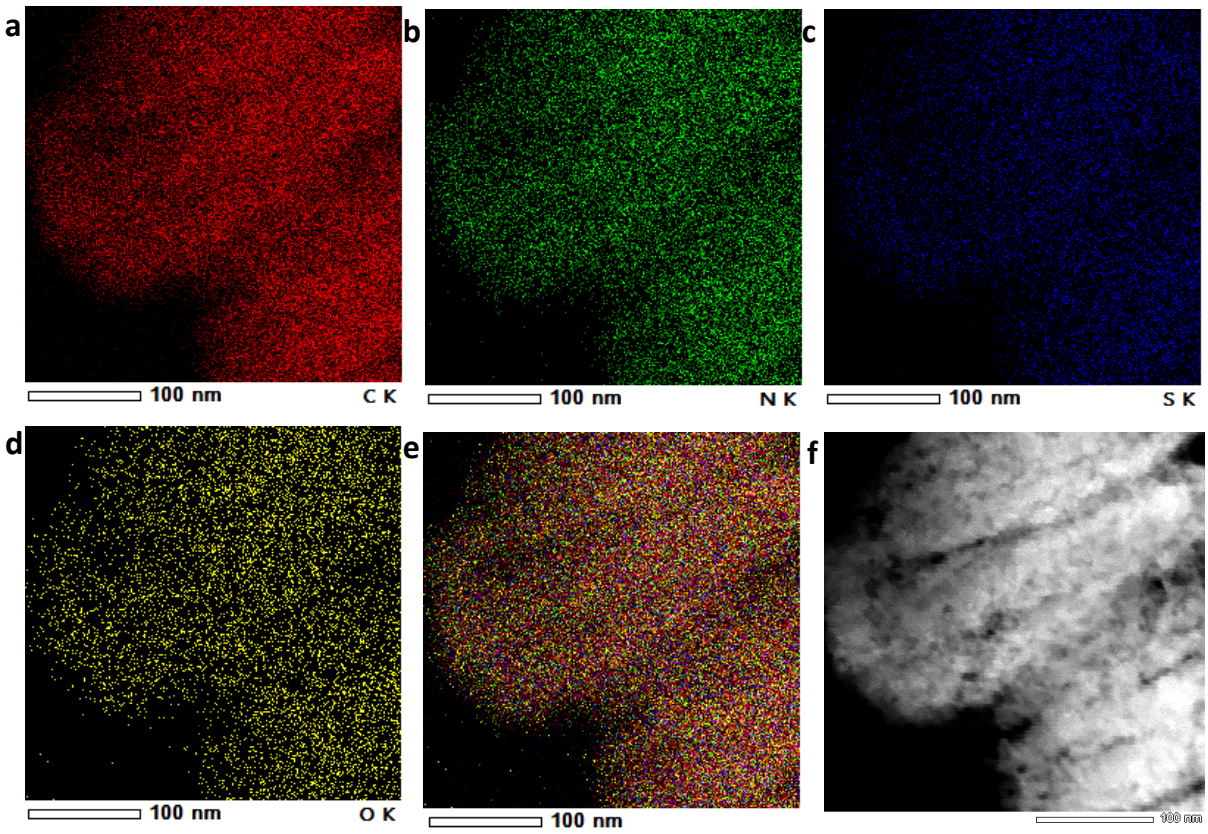


**Figure S19:** Elemental mapping of **NTB-DBT-80** after electrochemical studies.

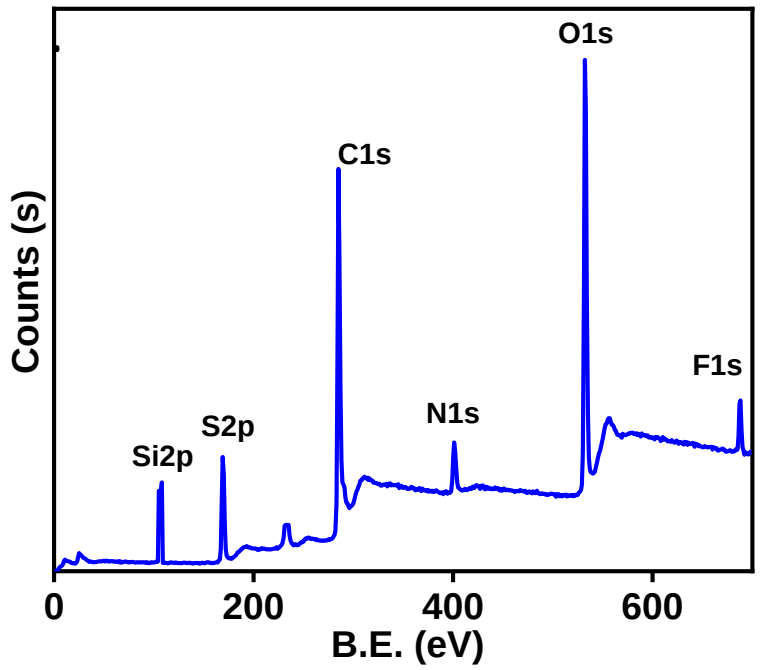


**Figure S20.** XPS of **NTB-DBT-80** after electrochemical studies.

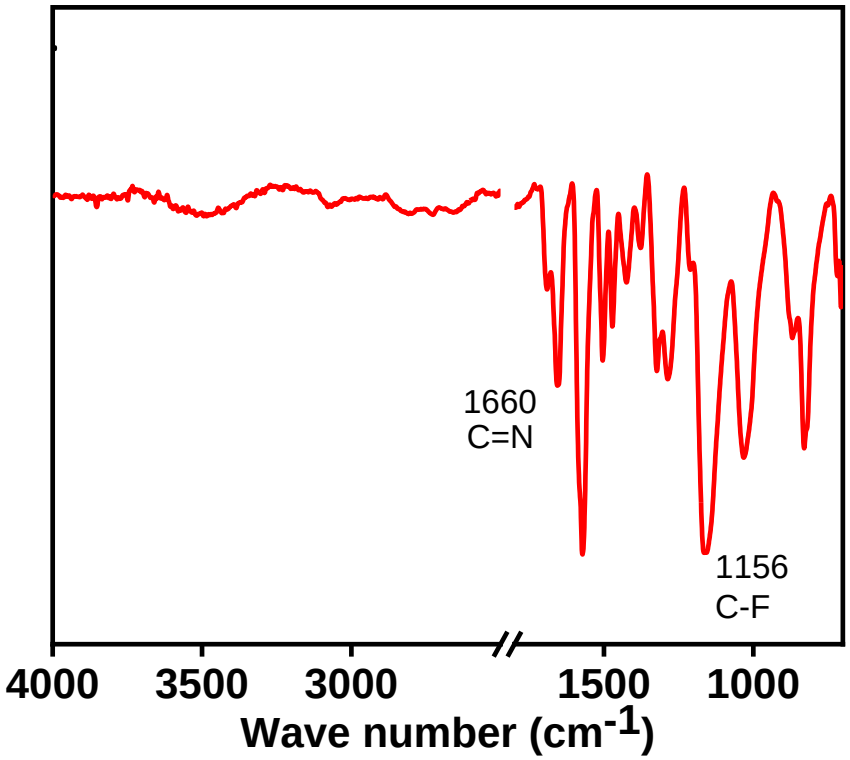


**Figure S21.** FT-IR spectra of **NTB-DBT-80** after electrochemical studies.

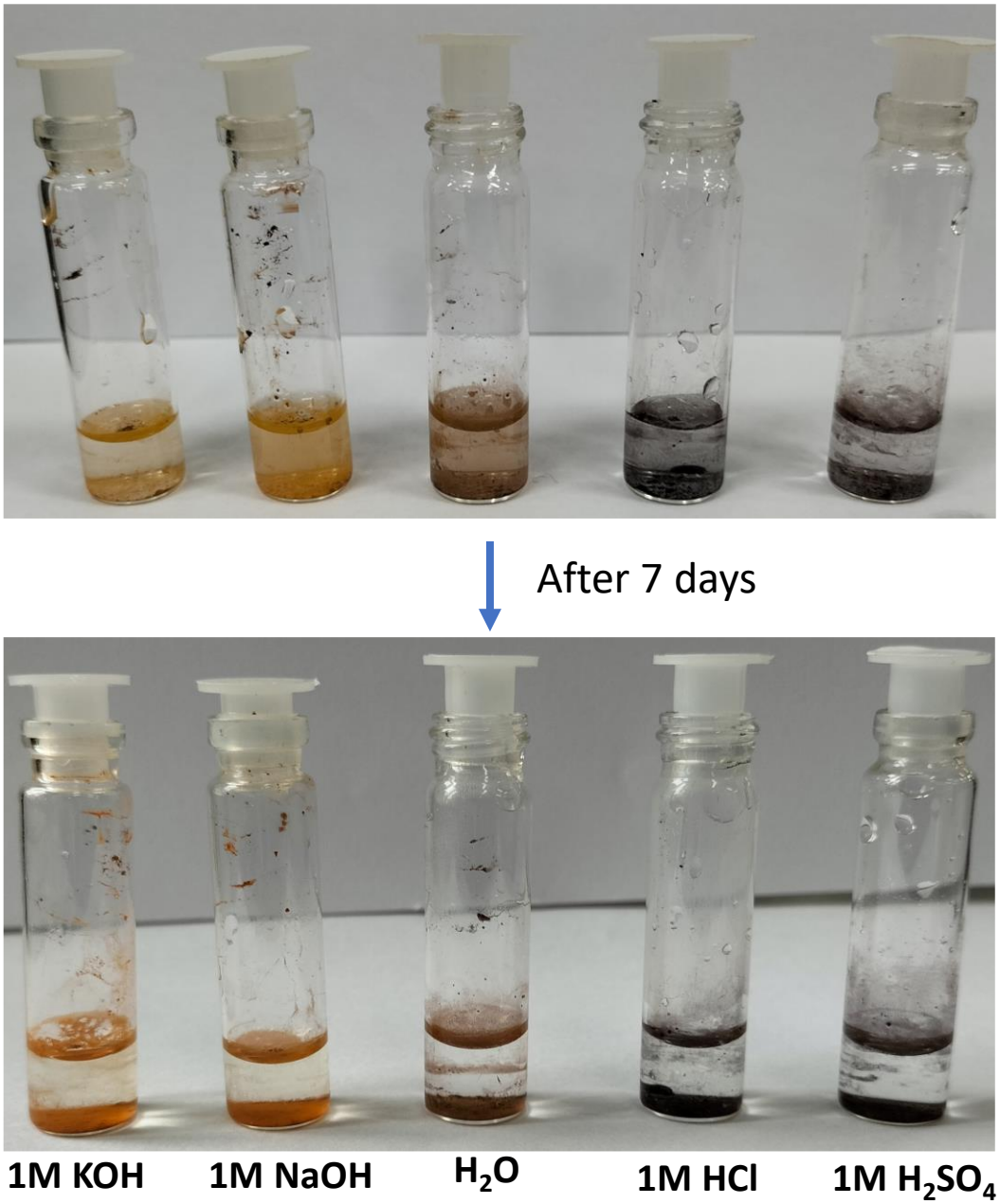


**Figure S22.** Images of NTB-DBT dispersed in 1M KOH, 1M NaOH, $H_2O$, 1M HCl, and 1M $H_2SO_4$.

**Table S1**. Comparison of 2D polymers based supercapacitors in a three-electrode system.

| S. No | Material | Gravimetric Capacitance ($F\ g^{-1}$) | Current Density ($Ag^{-1}$) | Electrolyte | Cycles | Reference |
|---|---|---|---|---|---|---|
| 1. | **Graphene-based electrode** | 154.1 | 1 | $EMIMBF_4$ ionic liquid electrolyte | _ | *Nano Lett.* **2010**, 10, 4863 |
| 2. | **GNS/CB** | 175 | | 6 M KOH | 6000 | *Carbon* **2010**, 48, 1731 |
| 3. | **G-PNF$_{30}$** | 210 | 0.3 | 1 M $H_2SO_4$ | 800 | *ACS Nano*, **2010**, 4, 1963 |
| 4. | **DAAQ-TFP/carbon black** | 48 ± 10 | 0.1 | 1 M $H_2SO_4$ | 5000 | *J. Am. Chem. Soc.* **2013**, 135, 16821 |
| 5. | **[TEMPO]100% NiP-COF** | 167 | 0.5 | 0.1 M $(C_4H_9)_4NClO_4$ | 100 | *Angew. Chem. Int. Ed*. **2015**, 54, 6814 |
| 6. | **Ni$_3$ (HITP)$_2$** | 111 | 0.05 | 1 M $TEABF_4$ /CAN. Mater | 10000 | *Nat. Mater*. **2017**, 16, 220 |
| 7. | **BIBDZ** | 88.4 | 0.5 | 1 M $H_3PO_4$ | 5000 | *Eur. Polym. J.* **2017**, 93, 448 |
| 8. | **TpOMe-DAQ** | 169 | 0.35 | 3 M $H_2SO_4$ | 100000 | *J. Am. Chem. Soc.* **2018**, 140, 10941 |
| 9. | **RGO-ACP$_3$** | 117 | 0.5 | 1 M $H_2SO_4$ | | *J. Power Sources*, **2020,** 450, 227611. |
| 10. | **POSS-F-POIP** | 36.2 | 0.5 | 1 M KOH | 2000 | *Microporous Mesoporous Mater.*, **2021**, 328, 111505. |
| 11. | **POSS-A-POIP** | 152.5 | 0.5 | 1 M KOH | 2000 | *Microporous Mesoporous Mater.*, **2021**, 328, 111505. |
| 12. | **Cz-TP CMP** | 67.38 | 1 | 1 M $H_2SO_4$ | | *Polym. J.*, **2022**, 254, 125070. |

| | | | | | | |
|---|---|---|---|---|---|---|
| 13. | **Cz-Cz CMP** | 43.70 | 0.5 | 1 M $H_2SO_4$ | | *Polym. J.*, **2022**, 254, 125070. |
| 14. | **a-COFs** | 115 | 0.1 | 1 M $H_2SO_4$ | 1000 | *Chemistry Select*, **2023**, 8, e202301774. |
| 15. | **NTB-DBT** | **217.84** | **0.1** | **1 M$H_2SO_4$** | **10000** | ***This work*** |

## Reference


S1. X. Wang, L. Chen, S. Y. Chong, M. A. Little, Y. Wu, W.-H. Zhu, R. Clowes, Y. Yan, M. A. Zwijnenburg, R. S. Sprick and A. I. Cooper, *Nat. Chem.*, 2018, **10**, 1180-1189.

S2. K. Geng, T. He, R. Liu, S. Dalapati, K. T. Tan, Z. Li, S. Tao, Y. Gong, Q. Jiang and D. Jiang, *Chem. Rev.*, 2020, **120**, 8814-8933

S3. X. Yan, T. Xu, G. Chen, S. Yang, H. Liu and Q. Xue, *J. Phys. D: Appl. Phys.*, 2004, **37**, 907-913.

S4. S. K. Das, C. Dickinson, F. Lafir, D. F. Brougham and E. Marsili, *Green Chem.*, 2012, **14**, 1322.

S5. Z. Huang, H. Chen, L. Zhao, W. Fang, X. He, W. Li and P. Tian, *Environ. Int.*, 2019, **126**, 289-297.